J. Fluid Mech. (2008), *vol.* 610, *pp.* 407–423.
doi:10.1017/S0022112008002772 Printed in the United Kingdom

Surfactant- and elasticity-induced inertialess instabilities in vertically vibrated liquids

BALRAM SUMAN AND SATISH KUMAR

Department of Chemical Engineering and Materials Science, University of Minnesota, Minneapolis, MN 55455, USA

(Received 5 September 2007 and in revised form 24 May 2008)

We investigate instabilities that arise when the free surface of a liquid covered with an insoluble surfactant is vertically vibrated and inertial effects are negligible. In the absence of surfactants, the inertialess Newtonian system is found to be stable, in contrast to the case where inertia is present. Linear stability analysis and Floquet theory are applied to calculate the critical vibration amplitude needed to excite the instability and the corresponding wavenumber. A previously reported long-wavelength instability is found to persist to finite wavelengths, and the connection between the long-wavelength and finite-wavelength theories is explored in detail. The instability mechanism is also probed and requires the Marangoni flows to be sufficiently strong and in the appropriate phase with respect to the gravity modulation. For viscoelastic liquids, we find that instability can arise even in the absence of surfactants and inertia. Mathieu equations describing this are derived and these show that elasticity introduces an effective inertia into the system.

1. Introduction

The effect of surfactants on interfacial hydrodynamics has long been a topic of study due to its importance in nature and industry. Yet in spite of numerous investigations, novel and fascinating phenomena continue to be uncovered even in relatively simple flows. One of the most remarkable observations is that surfactants can destabilize a flow that would be completely stable (to small-amplitude disturbances) in the absence of surfactants. In particular, it was recently discovered that surfactants can destabilize the inertialess flow of two adjacent fluids in a channel, a system for which no instability exists when surfactants are absent (Frenkel & Halpern 2002; Halpern & Frenkel 2003; Blyth & Pozrikidis 2004; Wei 2007). Surfactants can also induce instabilities in liquid droplets that spread on an underlying liquid layer (Troian, Wu & Safran 1989; Warner, Craster & Matar 2004; Edmonstone, Craster & Matar 2006). The purpose of this contribution is to discuss another example of an otherwise stable system that is destabilized by surfactants: the free surface of an inertialess vertically vibrated liquid.

It is well known that in the presence of inertia, a vertically vibrated liquid free surface can become unstable, giving rise to Faraday waves (Faraday 1831; Benjamin & Ursell 1954; Kumar 1996)). The effects of insoluble surfactants on this instability have recently been accounted for through linear stability analysis (Kumar & Matar 2004*a*, *b*; Giavedoni & Ubal 2007) and numerical simulations (Ubal, Giavedoni & Saita 2005*a*, *b*, *c*). In addition to these studies, which analyse the full Navier–Stokes equations, a model based on the lubrication approximation has been developed and

investigated (Kumar & Matar 2002; Matar, Kumar & Craster 2004). In this model, which is strictly valid for long-wavelength disturbances, inertia was absent and it was found that instability could not occur in the absence of surfactants. However, once surfactants are present, instability can occur thanks to the Marangoni flows engendered by surfactant concentration gradients.

Although the effects of surfactants on the Faraday instability have been previously examined, several outstanding questions remain. First, does the inertialess instability reported in Kumar & Matar (2002) persist for finite-wavelength disturbances? Studies of Faraday waves of finite wavelengths have generally focused on cases where inertial effects are significant; the inertialess case appears to have been overlooked. Second, how well does the long-wavelength theory work compared to the finite-wavelength theory? Connections between the two theories were not attempted in prior work (Kumar & Matar 2002; Matar *et al.* 2004). Third, what is the mechanism for the surfactant-induced destabilization? This has been probed to some extent in Matar *et al.* (2004), but only in the long-wavelength limit and for a limited range of parameters. The above questions will be addressed in the present work. In addition, we investigate the effect of liquid viscoelasticity and find that it can cause a vertically vibrated liquid free surface to become unstable even in the absence of surfactants and inertia.

The governing equations are presented in § 2, the inertialess Newtonian limit is examined in detail in § 3, and Floquet theory is applied in § 4. Results and discussions for Newtonian and viscoelastic liquids are given in § 5 and § 6, respectively, with conclusions following in § 7.

2. Governing equations

We consider an incompressible liquid on top of a horizontal plate of infinite length and width. The plate is vertically vibrated in a sinusoidal fashion with an acceleration of amplitude a and frequency ω. The reference frame is fixed to the plate, which is in the (x, y)-plane and located at $z = -h$. No-slip and no-penetration boundary conditions apply at the plate, and in the reference frame adopted the base state is quiescent.

The free surface of the undisturbed liquid is covered with a monolayer of an insoluble surfactant and located at $z = 0$. The surfactant diffusion coefficient is denoted by D, σ_0 is the surface tension when surfactant is absent, and σ_m is the surface tension at the mean surfactant concentration. The surfactant concentration is assumed to obey a linear equation of state. The liquid is characterized by a density ρ, Newtonian solvent viscosity η_s, non-Newtonian contribution to the zero-shear viscosity η_p, and characteristic relaxation time λ.

As the derivation of the linearized governing equations has been presented elsewhere (Kumar 1999; Kumar & Matar 2004*a*, *b*; Suman 2008), we simply show the final result. The equations are given in non-dimensional form, where length is scaled with h, time with $1/\omega$, velocity with $h\omega$, pressure with $\eta_s\omega$, and surfactant concentration with Γ_m, the mean surfactant concentration. The linearized governing equations are:

$$(Re\,\partial_t - (\partial_{zz} - k^2))(\partial_{zz} - k^2)w - \frac{\eta}{De}\int_{-\infty}^{t} F(t-t')(\partial_{zz} - k^2)^2 w\,\mathrm{d}t' = 0, \tag{2.1}$$

$$(Re\,\partial_t - (\partial_{zz} - 3k^2))\partial_z w|_{z=0} - \frac{\eta}{De}\int_{-\infty}^{t} F(t-t')(\partial_{zz} - 3k^2)\partial_z w|_{z=0}\,\mathrm{d}t' + k^2\tilde{\mathscr{B}}(t)\zeta + Ck^4\zeta = 0, \tag{2.2}$$

$$\partial_t \Gamma - \partial_z w|_{z=0} + \frac{k^2}{Pe}\Gamma = 0, \tag{2.3}$$

$$\partial_t \zeta = w|_{z=0}, \tag{2.4}$$

$$(\partial_{zz} + k^2)w|_{z=0} + \frac{\eta}{De}\int_{-\infty}^{t} F(t-t')(\partial_{zz} + k^2)w|_{z=0}\, \mathrm{d}t' + Mk^2\Gamma = 0, \tag{2.5}$$

$$w|_{z=-1} = 0, \quad \partial_z w|_{z=-1} = 0, \tag{2.6}$$

where k is the magnitude of the wavevector in the (x, y)-plane, F is a relaxation modulus, ζ is the height of the perturbed free surface, w is the z-component of the liquid velocity, and Γ is the surfactant concentration. Note that here $\zeta = \zeta(t)$, $w = w(z, t)$, and $\Gamma = \Gamma(t)$ since these now represent the amplitudes of the normal modes. The dimensionless parameters that appear in the above equations include a Reynolds number, $Re \equiv \rho h^2\omega/\eta_s$, viscosity ratio, $\eta \equiv \eta_p/\eta_s$, Deborah number, $De \equiv \lambda\omega$, inverse capillary number, $C \equiv \sigma_m/\eta_s\omega h$, Péclet number, $Pe \equiv h^2\omega/D$, and Marangoni number, $M \equiv (\sigma_o - \sigma_m)/\eta_s\omega h$. In addition, $\tilde{\mathscr{B}}(t) = B - \tilde{A}\cos(t)$ with $B \equiv \rho g h/\eta_s\omega$ and $\tilde{A} \equiv \rho a h/\eta_s\omega$, where g is the mean acceleration due to gravity.

3. Inertialess Newtonian limit

We now consider the case in which inertial and viscoelastic effects are absent, i.e. $Re = 0$ and $\eta = 0$, in order to connect our analysis with that of Kumar & Matar (2002), who analysed long-wavelength disturbances on vertically vibrated thin liquid films. Equation (2.1) simplifies to:

$$(\partial_{zz} - k^2)^2 w = 0, \tag{3.1}$$

which can be solved to yield:

$$w(z, t) = (P + Qz)\cosh(kz) + (R + Sz)\sinh(kz), \tag{3.2}$$

where P, Q, R, and S are functions of t but not z. Equation (2.6) can be used to obtain Q and R in terms of P and S:

$$Q = \frac{\sinh^2(k)S - kP}{\sinh(k)\cosh(k) - k}, \quad R = \frac{\cosh^2(k)P - kS}{\sinh(k)\cosh(k) - k}. \tag{3.3}$$

Similarly, equation (2.5) gives:

$$S = \frac{-Mk\Gamma}{2} - kP, \tag{3.4}$$

while equation (2.4) gives:

$$P = \zeta_t. \tag{3.5}$$

Application of equation (2.2) produces:

$$2kR + (\tilde{\mathscr{B}}(t) + Ck^2)\zeta = 0, \tag{3.6}$$

which can be combined with (3.3) to (3.5) to obtain a first-order ordinary differential equation (ODE) for ζ:

$$2k\left(\frac{\cosh^2(k) + k^2}{\sinh(k)\cosh(k) - k}\right)\zeta_t + (\tilde{\mathscr{B}}(t) + Ck^2)\zeta + \left(\frac{k^3}{\sinh(k)\cosh(k) - k}\right)M\Gamma = 0. \tag{3.7}$$

A corresponding equation for Γ can be obtained by combining (2.3) with (3.2) to (3.5):

$$\Gamma_t - \frac{k^3}{\sinh(k)\cosh(k) - k}\zeta_t + \left[\left(\frac{\sinh^2(k) - k^2}{\sinh(k)\cosh(k) - k}\right)\frac{Mk}{2} + \frac{k^2}{Pe}\right]\Gamma = 0. \tag{3.8}$$

Equations (3.7) and (3.8) are a coupled system of first-order ODEs describing the free-surface height and surfactant concentration perturbation. If the left-hand sides of these equations are Taylor expanded around $k = 0$ and only the leading-order terms retained, one recovers equations equivalent to those in Kumar & Matar (2002), which were derived by direct application of the lubrication approximation to the governing equations. Equations (3.7) and (3.8) thus generalize the results of Kumar & Matar (2002) for arbitrary wavelengths. These equations may exhibit instability, and this will be probed in the next section through application of Floquet theory. Before doing so, we consider several other limits.

When surfactant effects are absent, i.e. $\Gamma = 0$ or $M = 0$, equation (3.7) reduces to:

$$2k\left(\frac{\cosh^2(k) + k^2}{\sinh(k)\cosh(k) - k}\right)\zeta_t + (\tilde{\mathscr{B}}(t) + Ck^2)\zeta = 0, \tag{3.9}$$

which can be solved to yield:

$$\zeta(t) = \zeta(0)\exp\left[\left(\frac{\cosh(k)\sinh(k) - k}{2k\left(\cosh^2(k) + k\right)}\right)\left(-(B + Ck^2)t - \frac{\tilde{A}\sin(\omega t)}{\omega}\right)\right]. \tag{3.10}$$

Equation (3.10) reveals that $\zeta \to 0$ as $t \to \infty$ no matter how large $\tilde{A}$ is. Thus, the free surface of a vertically vibrated Newtonian liquid is stable if inertia and surfactants are absent. The same conclusion was drawn by Kumar & Matar (2002) for the case of long-wavelength disturbances.

In the opposite limit, $M \to \infty$, one finds that $\Gamma = 0$ as $M \to \infty$, meaning that this case is stable too. Returning to equation (2.5), one also sees here that $\Gamma = 0$ as $M \to \infty$, and using this result in equation (2.3) implies that $\partial_z w|_{z=0} = 0$. If we consider just the (x, z)-plane, the continuity equation then requires that $\partial_x u|_{z=0} = 0$, where u is the dimensionless horizontal velocity component. This result implies that the free surface neither contracts nor expands, and that it is a no-slip surface ($u|_{z=0} = 0$). However, the surface can still deform in the vertical direction. This is a so-called inextensible surface, which was considered by Lamb in modelling the calming effect of oil on water waves (Lamb 1932). One can also consider a limit in which $M \to \infty$ but $\Gamma M = O(1)$, but it is readily shown that this leads to a first-order ODE in ζ which is stable.

For the case of an infinite-depth surfactant-covered liquid, modified forms of equations (3.7) and (3.8) can be obtained by replacing (2.6) with:

$$w|_{z=-\infty} = 0, \qquad \partial_z w|_{z=-\infty} = 0. \tag{3.11}$$

In this case, the length scale $\sqrt{\sigma_o/\rho g}$ has been used for non-dimensionalization. From equation (2.1), we obtain:

$$w(z, t) = (P + Qz)\exp(kz), \tag{3.12}$$

where P and Q are functions of t but not z. The modified boundary conditions give:

$$P = \zeta_t, \tag{3.13}$$

$$Q = \frac{-Mk\Gamma}{2} - k\zeta_t. \tag{3.14}$$

Equation (3.6) then yields:

$$2k\zeta_t + (\tilde{\mathscr{B}}(t) + Ck^2)\zeta = 0, \tag{3.15}$$

while equation (2.3) gives:

$$\Gamma_t + \left(\frac{Mk}{2} + \frac{k^2}{Pe}\right)\Gamma = 0. \tag{3.16}$$

Note that equations (3.15) and (3.16) are decoupled as the normal stress balance along with the no-slip and kinematic boundary conditions yields equation (3.15), and the surfactant transport equation along with the no-penetration boundary condition and shear stress balance gives (3.16). Indeed, if one considers the limit of infinite liquid depth, it can be shown that the last term of (3.7) and the second term of (3.8) become zero, reducing those equations to (3.15) and (3.16).

The latter two equations can be solved to give:

$$\zeta(t) = \zeta(0)\exp\left[\left(\frac{1}{2k}\right)\left(-(B + Ck^2)t - \frac{\tilde{A}\sin(\omega t)}{\omega}\right)\right], \tag{3.17}$$

$$\Gamma(t) = \Gamma(0)\exp\left[-\left(\frac{Mk}{2} + \frac{k^2}{Pe}\right)t\right], \tag{3.18}$$

which indicate that as $t \to \infty$, $\zeta \to 0$ and $\Gamma \to 0$. Thus, the vertically vibrated free surface of a Newtonian liquid of infinite depth is stable in the absence of inertia even if surfactants are present. It is noteworthy that in this limit, two of the natural length scales in the problem, h (the liquid depth) and $\sqrt{\nu/\omega}$ (the viscous penetration depth), are infinite. In the presence of inertia, the latter length scale is finite and instability can occur in the absence of surfactants even for an infinite-depth liquid. When viscous effects are weak, the surface height is well-described by a damped Mathieu equation (Kumar & Tuckerman 1994). (Even when viscous effects are not weak and inertia is present, a Mathieu equation can be derived for the surface height under some conditions (Cerda & Tirapegui 1998; Cerda, Rojas & Tirapegui 2000).) In the absence of inertia, instability appears to require the former length scale to be finite and the presence of surfactants. The dynamics of the surfactant couple with those of the surface height to yield a second-order ODE for ζ, as can be seen by differentiating equation (3.7) and substituting (3.8). The potential of this coupled system to exhibit instability is discussed next.

4. Floquet theory

Since the forcing in the problem is time-periodic, Floquet theory can be applied to analyse the linear stability problem presented by equations (2.1) to (2.6). We again consider the inertialess limit ($Re = 0$) but allow for viscoelastic effects ($\eta \neq 0$). We first express $\zeta(t)$, $w(z, t)$, and $\Gamma(t)$ as time-periodic functions:

$$\zeta(t) = \exp((s + \mathrm{i}\alpha)t)\sum_{-\infty}^{\infty}\zeta_n \exp(\mathrm{i}nt), \tag{4.1}$$

$$w(z, t) = \exp((s + \mathrm{i}\alpha)t)\sum_{-\infty}^{\infty}w_n(z)\exp(\mathrm{i}nt), \tag{4.2}$$

$$\Gamma(t) = \exp((s + \mathrm{i}\alpha)\, t) \sum_{-\infty}^{\infty} \Gamma_n \exp(\mathrm{i}nt), \tag{4.3}$$

where s is a real-valued growth rate. The value of α determines the temporal nature of the surface response; $\alpha = 0$ corresponds to a harmonic response whereas $\alpha = 1/2$ corresponds to a subharmonic response. Consistent with prior studies (Kumar 1999; Kumar & Matar 2004*a*, *b*), only these two values of α are considered.

Substituting equation (4.2) into (2.1), we obtain:

$$(\partial_{zz} - k^2)^2 w_n(z) = 0, \tag{4.4}$$

and $w_n(z)$ can be expressed as:

$$w_n(z) = (P_n + Q_n z)\cosh(kz) + (R_n + S_n z)\sinh(kz), \tag{4.5}$$

where P_n, Q_n, R_n, and S_n are constants. From equations (2.6) and (4.5), Q_n and R_n are found to be:

$$Q_n = \frac{\sinh^2(k) S_n - k P_n}{\sinh(k)\cosh(k) - k}, \qquad R_n = \frac{\cosh^2(k) P_n - k S_n}{\sinh(k)\cosh(k) - k}, \tag{4.6}$$

while equations (2.5), (4.3), and (4.5) give S_n as:

$$S_n = \frac{-Mk\Gamma_n}{2\nu_n} - kP_n, \tag{4.7}$$

where $\nu_n = 1 + (\eta/De)\int_0^{\infty} F(\tau)\mathrm{e}^{-(s+\mathrm{i}(\alpha+n))\tau}\,\mathrm{d}\tau$ with $\tau = t - t'$. Equations (2.4), (4.1), and (4.5) can be used to find P_n:

$$P_n = (s + \mathrm{i}(\alpha + n))\,\zeta_n. \tag{4.8}$$

With the help of (4.5), equation (2.2) becomes:

$$2k\nu_n R_n + (\tilde{\mathscr{B}}(t) + Ck^2)\zeta = 0. \tag{4.9}$$

Substituting the expression for R_n, we obtain the following relationship:

$$A_n\zeta_n + B_n\Gamma_n = \frac{\tilde{A}}{2}(\zeta_{n+1} + \zeta_{n-1}), \tag{4.10}$$

where

$$A_n = B + Ck^2 + 2k\nu_n\left(\frac{\cosh^2(k) + k^2}{\cosh(k)\sinh(k) - k}\right)(s + \mathrm{i}(\alpha + n)), \tag{4.11}$$

$$B_n = \frac{k^3 M}{\cosh(k)\sinh(k) - k}. \tag{4.12}$$

If equations (4.1) to (4.8) are combined with (2.3), another relationship results:

$$\Gamma_n = \gamma_n\zeta_n, \tag{4.13}$$

where

$$\gamma_n = \frac{k^3(s + \mathrm{i}(\alpha + n))}{(\cosh(k)\sinh(k) - k)(s + \mathrm{i}(\alpha + n) + k^2/Pe) + (\sinh^2(k) - k^2)kM/(2\nu_n)}. \tag{4.14}$$

Equations (4.10) to (4.14) form a recursion relation for the Fourier modes of the free-surface height and surfactant concentration perturbation. Kumar & Matar (2004*a*, *b*) developed a recursion relation for non-zero Re. In the limit that $Re \to 0$, application

of L'Hôpital's rule shows that their expressions reduce to equations (4.10) to (4.14). A similar argument holds in the infinite-depth case, where their recursion relation (when converted back to the time domain) becomes equivalent to equations (3.15) and (3.16) as $Re \to 0$.

The expression for $A_n + \gamma_n B_n$ can be rearranged to obtain:

$$A_n + \gamma_n B_n = B + Ck^2 + 3(s + \mathrm{i}(\alpha + n))\left[C_1 C_2 + \frac{C_1 M}{(s + \mathrm{i}(\alpha + n)) + k^2/Pe + C_3 Mk/(2\nu_n)}\right], \quad (4.15)$$

where

$$C_1 = \frac{k^6}{3(\cosh(k)\sinh(k) - k)^2}, \quad (4.16)$$

$$C_2 = \frac{2\nu_n(\cosh^2(k) + k)(\cosh(k)\sinh(k) - k)}{k^5}, \quad (4.17)$$

$$C_3 = \frac{\sinh^2(k) - k^2}{\cosh(k)\sinh(k) - k}. \quad (4.18)$$

Taking $\nu_n = 1$ (Newtonian liquid), Taylor expanding C_1, C_2, and C_3 around $k = 0$, and considering only leading-order terms gives $C_1 \approx 3/4$, $C_2 \approx 4/(3k^2)$, and $C_3 \approx k/2$. Here k is a small dimensionless wavenumber. This implies:

$$A_n + \gamma_n B_n = B + Ck^2 + 3(s + \mathrm{i}(\alpha + n))\left[\frac{1}{k^2} + \frac{3M}{4(s + \mathrm{i}(\alpha + n)) + k^2/Pe + Mk^2}\right]. \quad (4.19)$$

This expression is equivalent to the corresponding expression in Kumar & Matar (2002) (called A_n therein) obtained via application of the lubrication approximation to the governing equations.

In the Newtonian case, equations (4.10) to (4.14) have a relatively compact form when converted to the time domain:

$$2k\left(\frac{\cosh^2(k) + k^2}{\cosh(k)\sinh(k) - k}\right)\zeta_{tt} + \left[\tilde{\mathscr{B}}(t) + Ck^2 + \frac{k^6 M}{(\cosh(k)\sinh(k) - k)^2} + \left(\frac{\cosh^2(k) + k^2}{\cosh(k)\sinh(k) - k}\right) \times \left(\frac{k^2}{Pe} + \frac{(\sinh^2(k) - k^2)kM}{2(\cosh(k)\sinh(k) - k)}\right)\right]\zeta_t + \left[\left(\frac{k^2}{Pe} + \frac{(\sinh^2(k) - k^2)kM}{2(\cosh(k)\sinh(k) - k)}\right)(\tilde{\mathscr{B}}(t) + Ck^2) + \tilde{\mathscr{B}}_t(t)\right]\zeta = 0, \quad (4.20)$$

$$(\sinh(k)\cosh(k) - k)\,\Gamma_t + \left[(\sinh^2(k) - k^2)\frac{Mk}{2} + (\sinh(k)\cosh(k) - k)\frac{k^2}{Pe}\right]\Gamma = k^3\zeta_t, \quad (4.21)$$

where $\mathscr{B}_t(t)$ is the time derivative of $\mathscr{B}(t)$. These equations are derived assuming that the liquid is of finite depth and that $M \neq 0$. They can also be directly obtained from equations (3.7) and (3.8). It is seen that the free-surface height obeys a Mathieu equation, and that it acts as a forcing term in the equation governing the surfactant concentration perturbation. The Marangoni, Péclet and inverse capillary numbers

appear in both the damping and restoring terms in the Mathieu equation, as does the gravity modulation, giving rise to a time-dependent damping.

The recursion relation given by equations (4.10) to (4.14) can be truncated at a finite value of n ($n = 20$ is more than sufficient for the calculations reported herein) to form a matrix eigenvalue problem which can then be solved using standard numerical methods (Kumar & Tuckerman 1994). Setting $s = 0$ yields information about neutral stability, allowing one to obtain the critical vibration amplitude needed for instability, $\tilde{A}_c$, and the corresponding wavenumber, k_c, as functions of the other problem parameters.

5. Results and discussion: Newtonian case

Figure 1 shows $\tilde{A}_c$ and k_c for the Newtonian case ($\eta = 0$) as a function of M at various values of Re. Also shown are results from the creeping-flow theory and long-wavelength approximation at the lowest value of Re. We note that all results for non-zero Re are calculated using the recursion relations valid for arbitrary Reynolds number (equations (37) to (47) of Kumar & Matar 2004*a*, *b*) and the technique described in § 4. Results from the long-wavelength theory are obtained by using equation (4.19) in place of (4.15). Further details about the neutral stability curves used to generate figure 1 can be found in Suman (2008). We now discuss the results displayed in figure 1.

When Re is relatively large, $\tilde{A}_c$ increases as M increases, reaches a maximum, and then slowly decreases to a constant value at large M (figure 1*a*). In contrast, k_c initially decreases, reaches a minimum, and then increases to a constant value at large M (figure 1*b*) (Kumar & Matar 2004*a*, *b*). In this case, the response of the surface waves at instability onset is subharmonic.

The presence of a maximum in the critical amplitude reflects the behaviour of the damping coefficient for unforced surface waves. As discussed by Lucassen (1968) and Lucassen-Reynders & Lucassen (1969), liquid surfaces covered by an insoluble surfactant can support the propagation of two types of waves, transverse and longitudinal. In the absence of surfactants, small-amplitude surface waves are transverse in character. The addition of surfactant imparts an elasticity to the surface that allows the propagation of another type of wave, one which is longitudinal in character. Lucassen observed that the damping coefficient exhibits a maximum with respect to surface elasticity when, at a given frequency, the wavenumbers of the transverse and longitudinal waves coincide. He ascribed the existence of the maximum to a resonance between the two surface waves, where the resonance acts to increase the velocity gradients near the surface and thus the viscous dissipation. Experiments indicate that the damping coefficient does indeed show a maximum with respect to surface elasticity, and that the wavenumber of the surface waves shows a minimum near the surface elasticity where the damping coefficient maximum occurs (Lucassen & Hansen 1966; Lucassen-Reynders & Lucassen 1969). If the surfactant is soluble and its diffusivity is sufficiently large, the maximum in the damping coefficient will disappear (Lucassen & Hansen 1967; Decent 1997). For insoluble surfactants, increasing the surface diffusivity causes the maximum in $\tilde{A}_c$ to disappear (Kumar & Matar 2004*a*, *b*). Further references concerning the behaviour of unforced surface waves can be found in Henderson (1998).

As Re decreases, $\tilde{A}_c$ increases due to the higher level of viscous dissipation, and the response at instability onset switches to harmonic except at relatively small values of M ($M < \sim 1$). The maximum in the $\tilde{A}_c$ versus M curve shifts closer to the $M = 0$ axis,

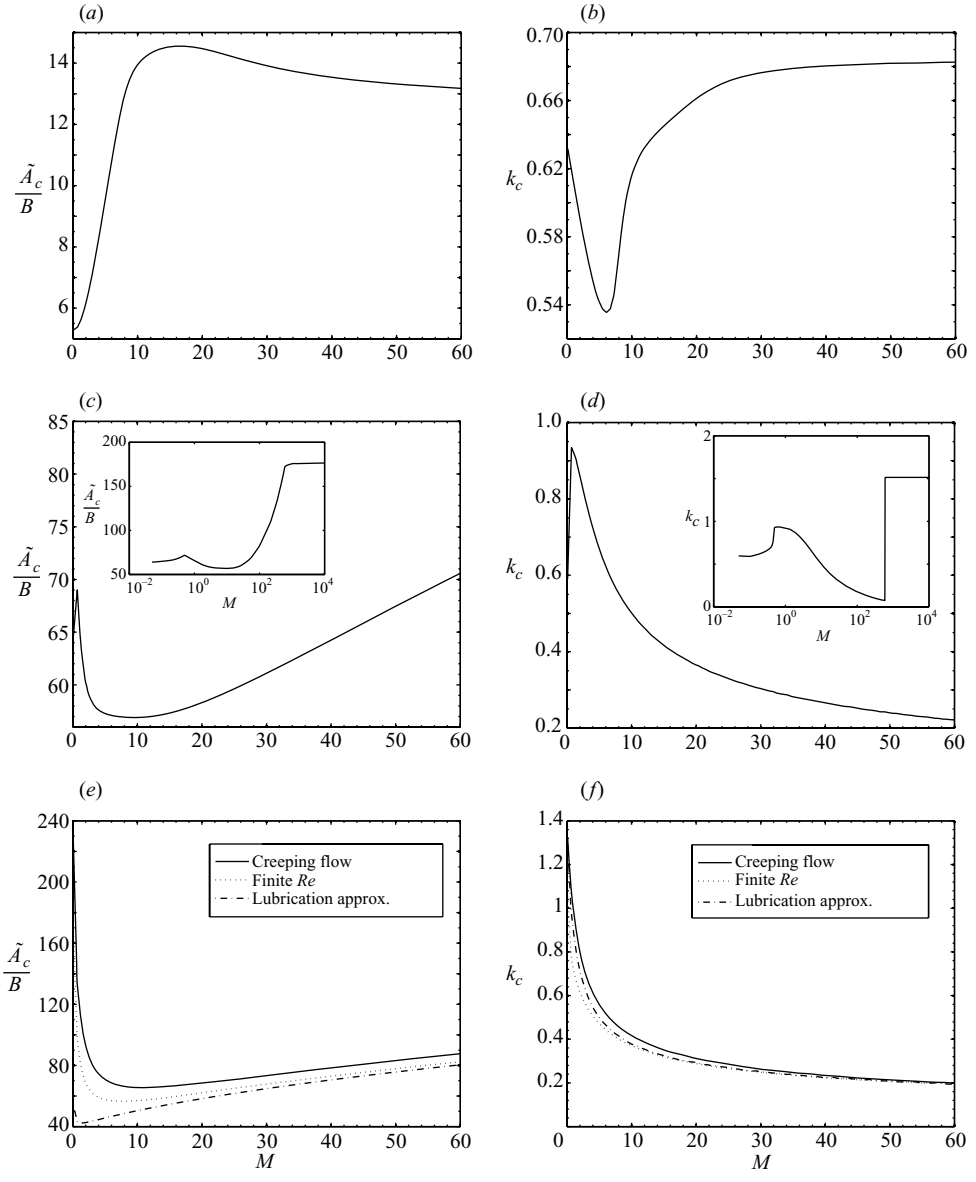

FIGURE 1. Critical amplitude, $\tilde{A}_c/B$, and wavenumber, k_c, versus M for (*a*), (*b*) $\eta_s = 0.05\,\mathrm{g\,cm^{-1}\,s^{-1}}$, $Re = 18.85$; (*c*), (*d*) $\eta_s = 0.4\,\mathrm{g\,cm^{-1}\,s^{-1}}$, $Re = 2.356$, (*e*), (*f*) $\eta_s = 1\,\mathrm{g\,cm^{-1}\,s^{-1}}$, $Re = 0.9425$. Other dimensional parameters are $\rho = 1\,\mathrm{g\,cm^{-3}}$, $\sigma_m = 30$ dyn cm^{-1}, $g = 981$ cm s^{-2}, $D = 10^{-4}$ cm^2 s^{-1}, $h = 0.5$ mm, and $\omega/2\pi = 60$ Hz; σ_o is varied to produce changes in M. The values of B range from 0.13 to 2.6, the values of C from 1.6 to 32, and $Pe = 9.4 \times 10^4$.

and the curve develops a minimum at finite M (figure 1*c*). As shown in the inset, $\tilde{A}_c$ still reaches a constant value at large M (corresponding to a no-slip surface). In addition, the minimum in the curve for k_c disappears and is replaced by a maximum, with k_c decreasing beyond that point (figure 1*d*). At sufficiently large M, k_c jumps to a new value (see inset) because of the existence of a bicritical point in the neutral stability curves; beyond this point, k_c and $\tilde{A}_c$ asymptote to constant values and the

system response remains harmonic. The maximum in the curves for $\tilde{A}_c$ and k_c near $M=0$ occurs at the point where the system response shifts from subharmonic to harmonic.

At even lower Re, the maxima in $\tilde{A}_c$ and k_c occur at $M=0$ (figures 1*e* and 1*f*). The creeping-flow theory yields predictions of the same order of magnitude as the finite-Re theory. (The agreement between the two calculations improves as Re is decreased even further.) The long-wavelength approximation agrees well with the creeping-flow theory at larger values of M, with increasing deviations as M becomes smaller since k_c increases as M decreases. Note that in the creeping-flow theory and long-wavelength approximation, the system is predicted to be stable for $M=0$ and $M \to \infty$, so $\tilde{A}_c$ might be expected to exhibit a minimum at finite M. In contrast, instability can occur in the finite-Re theory even when $M=0$ or $M \to \infty$. We note that as M becomes sufficiently large, $\tilde{A}_c$ and k_c for the finite-Re theory approach constant values; the behaviour is similar to that shown in the inset of figures 1(*c*) and 1(*d*) so we do not show insets for this case. In both the long-wavelength approximation and the creeping-flow theory, $\tilde{A}_c$ and k_c continue to increase as M increases since no instability can occur in these cases as $M \to \infty$.

In order to gain insight into the instability mechanism in the creeping-flow limit, we can write equation (3.7) as:

$$k\left(\frac{\cosh^2(k)+k^2}{\sinh(k)\cosh(k)-k}\right)\frac{(\zeta^2)_t}{\zeta^2} = -(B+Ck^2)+\tilde{A}\cos(t)-\left(\frac{k^3}{\sinh(k)\cosh(k)-k}\right)M\frac{\Gamma}{\zeta}. \tag{5.1}$$

A similar strategy was employed by Matar *et al.* (2004) to study long-wavelength disturbances. Without loss of generality, we consider values of k for which the term in parentheses on the left-hand side of equation (5.1) is positive. It is then clearly seen from the first term on the right-hand side that the mean gravity and surface tension play stabilizing roles. The second term on the right-hand side indicates that the gravity modulation will be stabilizing over one-half of the oscillation cycle and destabilizing over the other half. The third term, corresponding to Marangoni effects, can be either stabilizing or destabilizing depending on the values of ζ and Γ.

Figure 2 shows the temporal behaviour of each of the terms in equation (5.1) for several different cases. These plots are obtained by numerically solving equations (3.7) and (3.8). We first consider figure 2(*b*), which corresponds to a neutrally stable situation. It is seen that the Marangoni term is predominantly positive over an oscillation period, indicating that Marangoni effects tend to be destabilizing on average. Note that for part of an oscillation period, both the gravity modulation and Marangoni terms are positive. During this time, the gravitational acceleration will tend to enhance growth of interfacial disturbances, akin to a Rayleigh–Taylor instability (Kumar 2000). Furthermore, the numerical solution of equations (3.7) and (3.8) shows that during this time, the surfactant concentration is depleted at wave crests and enhanced at wave troughs. This then leads to a Marangoni flow that drives liquid from the troughs to the crests, thereby reinforcing their growth. Over another part of the oscillation period, both the gravity modulation and Marangoni terms are negative, meaning that Marangoni flows will promote gravitational levelling. However, since the Marangoni term is predominantly positive, this stabilizing effect is weak relative to the destabilizing effect noted earlier. There will also be times when the signs of both terms are opposite to each other. Again, since the Marangoni term is predominantly

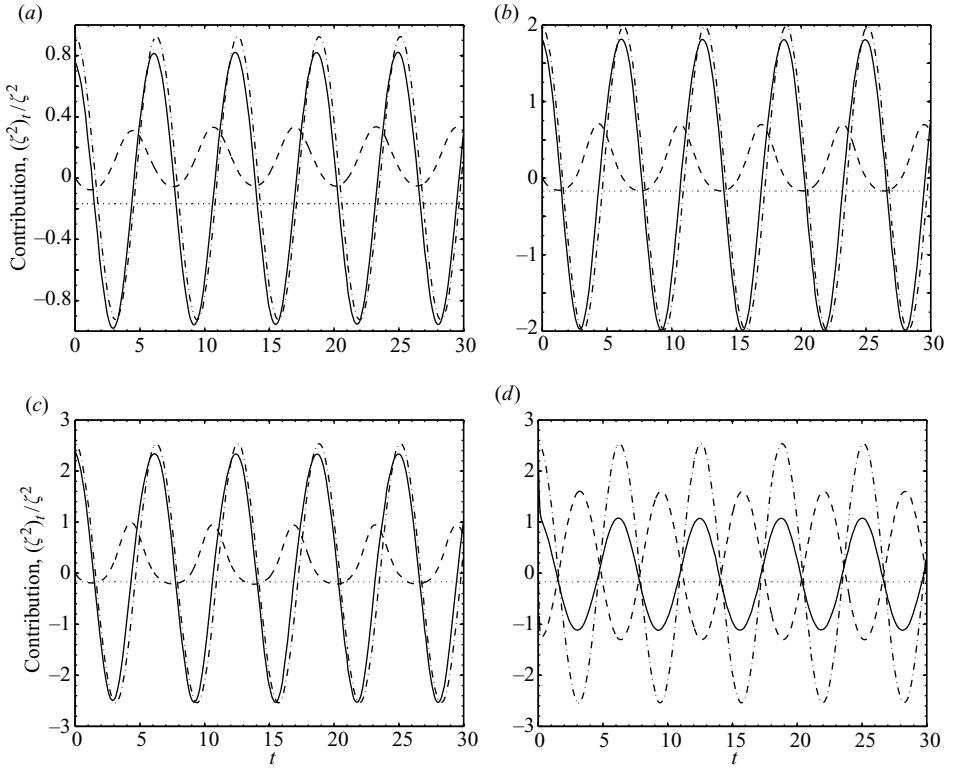

FIGURE 2. Temporal behaviour of various terms in equation (5.1): $(\zeta^2)_t/\zeta^2$ (solid line), mean gravity and surface tension term (dotted line), gravity modulation term (dashed-dotted line), Marangoni term (dashed line). We have taken $B = 0.13$, $C = 1.6$, $Pe = 9.4 \times 10^4$, and (*a*) $M = 1$, $\tilde{A} = 5$; (*b*) $M = 1$, $\tilde{A} = 11.1$; (*c*) $M = 1$, $\tilde{A} = 14.5$; (*d*) $M = 50$, $\tilde{A} = 14.5$.

positive, it will oppose gravitational levelling more than it hinders the Rayleigh–Taylor-type instability.

Figure 2(*a*) shows results for a lower value of $\tilde{A}$ than figure 2(*b*), and figure 2(*c*) shows results at a higher value, with all other parameters the same. These correspond to stable and unstable situations, respectively. Careful inspection shows that both the maximum and minimum values of the Marangoni term increase in magnitude as $\tilde{A}$ increases, but the maximum value increases more, tending to make the system more unstable. We note that the results in figure 2(*c*) may only reflect approximate behaviour since nonlinear effects may become important once the system is unstable. Figure 2(*d*) shows results at a higher value of M than figure 2(*c*) and corresponds to a stable situation. Although the amplitude of the Marangoni term is larger than in figure 2(*c*), it is negative for a longer portion of an oscillation period. In addition, the time during which both the Marangoni and gravity modulation terms are positive is smaller. It should also be noted that in some cases a stable system can be made unstable by increasing M, as can be inferred from figure 1(*e*). These results suggest that in order for instability to occur, the Marangoni term needs to be sufficiently large and positive during an oscillation period, and the time during which the Marangoni and gravity modulation terms are both positive must be sufficiently long.

Finally, we summarize the effects of varying the other problem parameters in the creeping-flow limit. As noted earlier, the mean gravity and surface tension play

stabilizing roles, so increases in B or C lead to increases in $\tilde{A}_c$. Increasing B also produces an increase in k_c, whereas increasing C produces a decrease in k_c. Decreasing Pe implies that surfactant diffusion becomes stronger, and as a consequence both $\tilde{A}_c$ and k_c increase. Since Marangoni forces become weaker as Pe decreases, all of the features in figure 1 (at any Re) tend to be flattened out, with $\tilde{A}_c$ and k_c becoming independent of M (Kumar & Matar 2004*a*; Giavedoni & Ubal 2007). Reducing Pe also decreases the magnitude of the Marangoni term in equation (5.1). Indeed, in the limit of vanishing Pe, it is straightforward to show that the system is always stable in the absence of inertia since Marangoni effects vanish in this limit.

The results of this section further clarify the mechanisms that can give rise to Faraday waves. When Re is relatively large, the instability mechanism is essentially inertial (i.e. the instability will occur even when $M=0$ or $M \to \infty$), although surfactants can have a significant effect on $\tilde{A}_c$ and k_c. This is the situation depicted in figures 1(*a*) and 1(*b*). When Re is relatively small, the instability mechanism at finite M primarily involves Marangoni effects, as shown by the good agreement between the creeping flow and finite-Re results in figures 1(*e*) and 1(*f*). Recall that in the creeping-flow limit, instability cannot occur unless Marangoni effects are present (which requires $0 < M < \infty$); the precise nature of the instability mechanism in this limit was discussed with reference to figure 2. If $M=0$ or $M \to \infty$, then the instability mechanism at low but non-zero Re will be inertial. For intermediate Reynolds numbers, both mechanisms play a role, as can be seen in figures 1(*c*) and 1(*d*), whose features are intermediate to those of figures 1(*a*, *b*) and 1(*e*, *f*).

6. Results and discussion: viscoelastic case

To investigate the effects of liquid viscoelasticity, we consider one of the simplest forms of the relaxation modulus, the single-mode Maxwell model (Bird, Armstrong & Hassager 1987; Larson 1988):

$$F(\tau) = \mathrm{e}^{-\tau/De}, \tag{6.1}$$

for which ν_n becomes:

$$\nu_n = 1 + \frac{\eta}{1 + De\,[s + \mathrm{i}(\alpha + n)]}. \tag{6.2}$$

Note that a Newtonian liquid is recovered in the limits $De \gg 1$ and $De \ll 1$. The most interesting behaviour occurs when $De \sim 1$, where the inertialess viscoelastic system can be unstable even when the corresponding Newtonian case is not.

We first consider the case of an infinite-depth liquid, for which the boundary conditions (3.11) hold. Carrying through the Floquet analysis of § 4 yields the following recursion relation:

$$(B + Ck^2 + 2k\nu_n\,[s + \mathrm{i}(\alpha + n)])\zeta_n = \frac{\tilde{A}}{2}\,(\zeta_{n+1} + \zeta_{n-1})\,, \tag{6.3}$$

which is decoupled from the surfactant-transport equation as in the Newtonian case. Although the surfactant concentration perturbation decays as before, the free surface can become unstable. Indeed, converting equation (6.3) back to the time domain yields:

$$2kDe\zeta_{tt} + [De(\tilde{\mathscr{B}}(t) + Ck^2) + 2k(1+\eta)]\zeta_t + (\tilde{\mathscr{B}}(t) + Ck^2 + De\tilde{\mathscr{B}}_t(t))\zeta = 0. \tag{6.4}$$

This is a Mathieu equation for the free-surface height in which the elasticity introduces an effective inertia. Although the system itself has no inertia, inertia-like effects can

arise since the liquid has a 'memory' of its prior deformations. Note that the inertial term is proportional to the Deborah number and is absent in the corresponding Newtonian case (cf. equation (3.15)). Furthermore, De, η, and C appear in the damping term, as does the gravity modulation, producing a time-dependent damping. In contrast, when true inertial effects are present, the Mathieu equation for a weakly damped Newtonian liquid of infinite depth has a constant damping proportional to the viscosity (Kumar & Tuckerman 1994).

For a finite-depth liquid in which surfactant effects are absent, one can obtain a recursion relation of the form (4.10) with $B_n = 0$ and:

$$A_n = B + Ck^2 + 2k\left(\frac{\cosh^2(k)+k^2}{\cosh(k)\sinh(k)-k}\right)\left(1+\frac{\eta}{1+De\,[s+\mathrm{i}(\alpha+n)]}\right)[s+\mathrm{i}(\alpha+n)]\,. \quad (6.5)$$

Converting back to the time domain yields the following Mathieu equation:

$$2k\left(\frac{\cosh^2(k)+k^2}{\cosh(k)\sinh(k)-k}\right)De\zeta_{tt} + \left[De(\tilde{\mathscr{B}}(t)+Ck^2)+2k\left(\frac{\cosh^2(k)+k^2}{\cosh(k)\sinh(k)-k}\right)(1+\eta)\right]\zeta_t + (\tilde{\mathscr{B}}(t)+Ck^2+De\tilde{\mathscr{B}}_t(t))\zeta = 0, \quad (6.6)$$

which is qualitatively similar to equation (6.4).

It is also possible to obtain a Mathieu equation for the finite-depth case in the limit $M \to \infty$ (no-slip or inextensible free surface). Here, A_n is the same as equation (6.5), but for $\gamma_n B_n$ we have

$$\gamma_n B_n = \frac{2k^5(s+\mathrm{i}(\alpha+s))}{(\cosh(k)\sinh(k)-k)(\sinh^2(k)-k^2)}\left(1+\frac{\eta}{1+De\,[s+\mathrm{i}(\alpha+n)]}\right). \quad (6.7)$$

The corresponding equation in the time domain is:

$$2k\left(\frac{\cosh^2(k)+k^2}{\cosh(k)\sinh(k)-k}+\frac{k^4}{(\cosh(k)\sinh(k)-k)(\sinh^2(k)-k^2)}\right)De\zeta_{tt} + \left[De(\tilde{\mathscr{B}}(t)+Ck^2)+\frac{2(1+\eta)k^5}{(\cosh(k)\sinh(k)-k)(\sinh^2(k)-k^2)} + \left(2k\left(\frac{\cosh^2(k)+k^2}{\cosh(k)\sinh(k)-k}\right)(1+\eta)\right)\right]\zeta_t + (\tilde{\mathscr{B}}(t)+Ck^2+De\tilde{\mathscr{B}}_t(t))\zeta = 0 \quad (6.8)$$

Equations (6.4), (6.6), and (6.8) are derived for $\eta \neq 0$ and finite De. Compared to (6.6), equation (6.8) has additional contributions in the inertial and damping terms. Note that the three inertialess cases considered above are all stable for Newtonian liquids, but could be unstable for viscoelastic liquids, a possibility that was overlooked in prior work.

For viscoelastic liquids of finite depth where surfactant effects are present, obtaining equations in the time domain is cumbersome, so we instead use equations (4.10) to (4.14) along with equation (6.2) to calculate the critical amplitude and wavenumber. Figure 3 shows how $\tilde{A}_c$ and k_c depend on M, De, and η. At low M, $\tilde{A}_c$ increases with

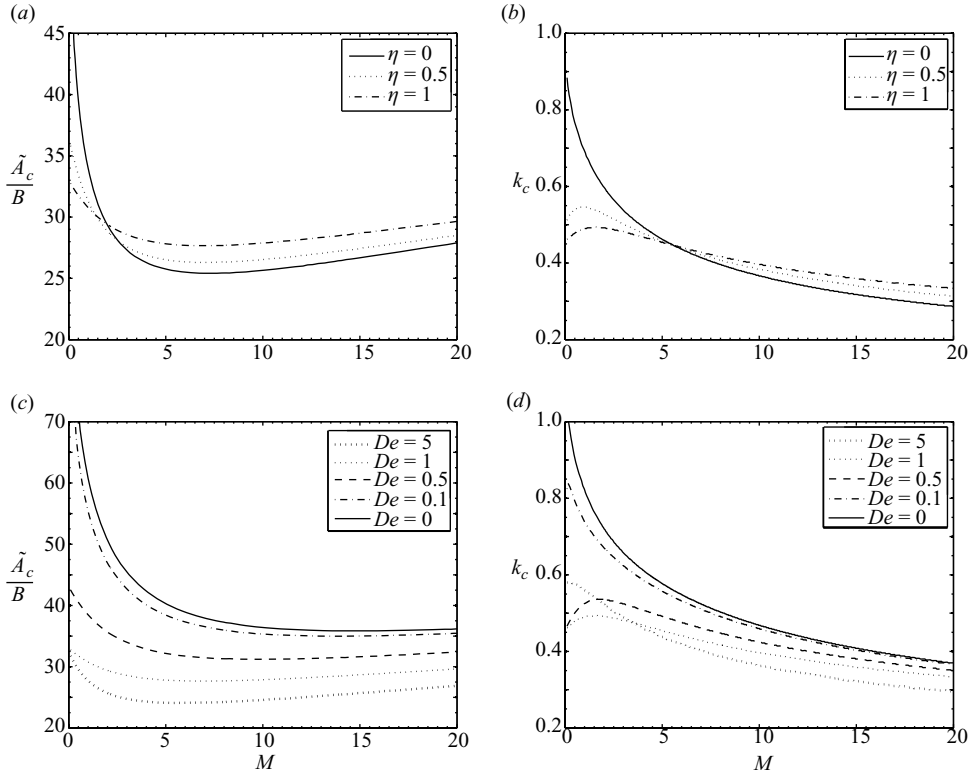

FIGURE 3. Critical amplitude, $\tilde{A}_c/B$, and wavenumber, k_c, versus M for $\rho = 1\,\mathrm{g\,cm^{-3}}$, $\sigma_o = 70\,\mathrm{dyn/cm}$, $\sigma_m = 30\,\mathrm{dyn/cm}$, $g = 981\,\mathrm{cm\ s^{-2}}$, $D = 10^{-4}\,\mathrm{cm^2/s}$, $h = 0.5\,\mathrm{mm}$, $\eta_s = 0.2\,\mathrm{g/(cm\,s)}$, and $\omega/2\pi = 60\,\mathrm{Hz}$: (*a*) and (*b*) $De = 1$; (*c*) and (*d*) $\eta = 1$. In all panels, $B = 0.65$, $C = 8$, and $Pe = 94250$.

a decrease in η. This can be understood by recognizing that when $M = 0$, the system is stable if viscoelastic effects are absent ($\eta = 0$; cf. § 3). Since $k_c \to \infty$ as $M \to 0$ when $\eta = 0$ (figure 1*f*), larger values of k_c occur as η decreases.

At higher M, $\tilde{A}_c$ increases with an increase in η. This can be understood by recognizing that the system can be unstable even in the Newtonian case, and that increasing η increases the level of viscous dissipation in the system. This dissipation will increase as η increases and is consistent with larger values of k_c. We note that at higher M, k_c decreases as M increases, similar to the Newtonian case. At low M, k_c increases as M increases for the non-zero values of η, evidently due to the presence of the elasticity-induced instability that operates in this regime.

Figure 3 shows that increasing De at higher M leads to a decrease in $\tilde{A}_c$ and k_c. This is due to a lowering of the effective viscosity in the system (cf. equation (6.2)). Although it is not evident from the plot, $\tilde{A}_c$, and as a result k_c, is a non-monotonic function of De at low M, becoming very large as $De \to \infty$ and $De \to 0$. This feature might be expected by noting that when surfactant effects are absent ($M = 0$), instability cannot occur unless viscoelastic effects are present, and that the liquid behaves as Newtonian when De is small or large. Because of this Newtonian behaviour at small and large De, k_c decreases as M increases at low M for small and large De. For intermediate De, where viscoelastic effects are present, k_c increases as M increases at low M, again due to the elasticity-induced instability that operates in

Situation	$\tilde{A}_c$	k_c
$\eta = 0, M = 0$	infinite	infinite
$\eta = 0, M \neq 0, Pe = 0$	infinite	infinite
$\eta = 0, 0 < M < \infty, Pe \neq 0$	finite	finite
$\eta = 0, M \to \infty$	infinite	zero
$\eta \neq 0, M = 0, De = 0$ or $De \to \infty$	infinite	infinite
$\eta \neq 0, M = 0, 0 < De < \infty$	finite	finite
$\eta \neq 0, M \neq 0, 0 < De < \infty$	finite	finite
$\eta \neq 0, 0 < M < \infty, Pe \neq 0, De = 0$ or $De \to \infty$	finite	finite
$\eta \neq 0, M \neq 0, Pe = 0, De = 0$ or $De \to \infty$	infinite	infinite

TABLE 1. Stability behaviour in the creeping-flow limit.

this regime. The behaviour of $\tilde{A}_c$ with respect to M for $De \neq 0$ is non-monotonic, similar to the Newtonian case. In all of the cases shown, the surface waves respond harmonically to the gravity modulation. Table 1 presents a summary of $\tilde{A}_c$ and k_c for a number of limiting cases in the creeping-flow limit.

The effects of the mean gravity and surface tension on $\tilde{A}_c$ and k_c for viscoelastic liquids are the same as those for Newtonian liquids. At higher M, the effect of Pe also remains unaltered by viscoelasticity. However, at low M, due to the presence of the elasticity-induced instability, decreasing Pe results in a decrease of k_c and an increase of $\tilde{A}_c$. Note that when $Pe = 0$, viscoelastic liquids can be unstable when inertia is absent, whereas Newtonian liquids cannot be.

7. Conclusions

We have explored an instability that is induced by surfactants when the free surface of a liquid is vertically vibrated and inertial effects are absent. The long-wavelength instability discovered by Kumar & Matar (2002) is found to persist even at finite wavelengths. Their long-wavelength theory can be recovered from the finite-wavelength theory developed here, and yields predictions that are in qualitative (and in some cases quantitative) agreement with the finite-wavelength theory. Instability requires the Marangoni flows to be sufficiently strong and in the appropriate phase with respect to the gravity modulation. In addition, we find that in viscoelastic liquids, instability can arise even in the absence of surfactants and inertia since the liquid elasticity gives rise to an effective inertia.

The present work answers several open questions from prior work and provides another example of how surfactants can destabilize a flow that is completely stable in their absence. It also presents a rather simple example of a purely elastic interfacial instability, given that elasticity can create instability in cases that would otherwise be stable in the inertialess Newtonian limit. Additional work should focus on the nonlinear regime of the instability, including pattern formation, as well as on Marangoni flows induced by temperature gradients (Birikh *et al.* 2001; Kumar, Bandyopadhyay & Mondal 2004; Mondal & Kumar 2006). Finally, we note that in addition to being of fundamental interest, Faraday waves have potential practical applications. Wright & Saylor (2003) have used Faraday waves in particle-laden thin liquid films to create patterned particulate deposits on a solid substrate. Takagi, Krinsky & Pumir (2002) have shown how Faraday waves can be used to influence the patterns that form in endothelial cell cultures. To the extent that each of these

applications potentially involves Marangoni and viscoelastic effects, the results of this study may be useful in designing Faraday waves to achieve a desired outcome.

REFERENCES

Benjamin, T. B. & Ursell, F. 1954 The stability of the plane free surface of a liquid in vertical periodic motion. *Proc. R. Soc. Lond.* A **225**, 505–515.

Bird, R. B., Armstrong, R. C. & Hassager, O. 1987 *Dynamics of Polymeric Liquids, Vol. 1. Fluid Mechanics*. Wiley.

Birikh, R. V., Briskman, V. A., Cherepanov, A. A. & Verlarde, M. G. 2001 Faraday ripples, parametric resonance and the Marangoni effect. *J. Colloid Interface Sci.* **238**, 16–23.

Blyth, M. G. & Pozrikidis, C. 2004 Effect of surfactants on the stability of two-layer channel flow. *J. Fluid Mech.* **505**, 59–86.

Cerda, E., Rojas, R. & Tirapegui, E. 2000 Asymptotic description of a viscous fluid layer. *J. Statist. Phys.* **101**, 553–565.

Cerda, E. A. & Tirapegui, E. L. 1998 Faraday's instability in a viscous fluid. *J. Fluid Mech.* **368**, 195–228.

Decent, S. P. 1997 The nonlinear damping of parametrically excited two-dimensional gravity waves. *Fluid Dyn. Res.* **19**, 201–217.

Edmonstone, B. D., Craster, R. V. & Matar, O. K. 2006 Surfactant-induced fingering phenomena beyond the critical micelle concentration. *J. Fluid Mech.* **564**, 105–138.

Faraday, M. 1831 On a peculiar class of acoustical figures; and on certain forms assumed by grups of particles upon vibrating elastic surfaces. *Phil. Trans. R. Soc. Lond.* **121**, 299–340.

Frenkel, A. L. & Halpern, D. 2002 Stokes-flow instability due to interfacial surfactant. *Phys. Fluids* **14**, L45–48.

Giavedoni, M. D. & Ubal, S. 2007 Onset of Faraday waves in a liquid layer covered with a surfactant with elastic and viscous properties. *Ind. Engng Chem. Res.* **46**, 5228–5237.

Halpern, D. & Frenkel, A. L. 2003 Destablization of a creeping flow by interfacial surfactant: linear theory extended to all wavenumbers. *J. Fluid Mech.* **485**, 191–220.

Henderson, D. M. 1998 Effects of surfactants on Faraday-wave dynamics. *J. Fluid Mech.* **365**, 89–107.

Kumar, K. 1996 Linear theory of Faraday instability in viscous liquids. *Proc. R. Soc. Lond.* A **452**, 1113–1126.

Kumar, K., Bandyopadhyay, A. & Mondal, G. C. 2004 Parametric instability in a fluid with temperature-dependent surface tension. *Europhys. Lett.* **65**, 330–336.

Kumar, K. & Tuckerman, L. S. 1994 Parametric instability of the interface between two fluids. *J. Fluid Mech.* **279**, 49–68.

Kumar, S. 1999 Parametrically driven surface waves in viscoelastic liquids. *Phys. Fluids* **11**, 1970–1981.

Kumar, S. 2000 Mechanism for the Faraday instability in viscous liquids. *Phys. Rev.* E **62**, 1416–1419.

Kumar, S. & Matar, O. K. 2002 Instability of long-wavelength distrbances on gravity-covered thin liquid layers. *J. Fluid Mech.* **466**, 249–258.

Kumar, S. & Matar, O. K. 2004*a* Erratum: On the Faraday instability in a surfactant-covered liquid. *Phys. Fluids* **16**, 3239–3239.

Kumar, S. & Matar, O. K. 2004*b* On the Faraday instability in a surfactant-covered liquid. *Phys. Fluids* **16**, 39–46.

Lamb, H. 1932 *Hydrodynamics*, 6th edn. Cambridge University Press.

Larson, R. G. 1988 *Constitutive Equations for Polymer Solutions and Melts*. Butterworths.

Lucassen, J. 1968 Longitudinal capillary waves. Part 1. Theory. *Trans. Faraday Soc.* **64**, 2221–2229.

Lucassen, J. & Hansen, R. S. 1966 Damping of waves on monolayer-covered surfaces. I. Systems with negligible surface dilational viscosity. *J. Colloid Interface Sci.* **22**, 32–44.

Lucassen, J. & Hansen, R. S. 1967 Damping of waves on monolayer-covered surfaces. II. Influence of bulk-to-surface diffusional interchange on ripple characteristics. *J. Colloid Interface Sci.* **23**, 319–328.

Lucassen-Reynders, E. H. & Lucassen, J. 1969 Properties of capillary waves. *Adv. Colloid Interface Sci.* **2**, 347–395.

Matar, O. K., Kumar, S. & Craster, R. V. 2004 Nonlinear parametrically excited surface waves in surfactant-covered thin liquid films. *J. Fluid Mech.* **520**, 243–265.

Mondal, G. C. & Kumar, K. 2006 Effect of Marangoni and coriolis forces on multicritical points in a Faraday experiment. *Phys. Fluids* **18**, 032101–1–9.

Suman, B. 2008 Continuum and molecular modeling of interfacial dynamics: Interfacial instabilities, melt spinning, and dendrimer adsorption. PhD thesis, University of Minnesota.

Takagi, S., Krinsky, V. & Pumir, A. 2002 The use of Faraday instability to produce defined topological organization in cultures of mammalian cells. *Intl J. Bifurcat. Chaos* **12**, 2009–2019.

Troian, S. M., Wu, X. L. & Safran, S. A. 1989 Fingering instability in thin wetting films. *Phys. Rev. Lett.* **62**, 1496–1499.

Ubal, S., Giavedoni, M. D. & Saita, F. A. 2005*a* Elastic effects of an insoluble surfactant on the onset of two-dimensional Faraday waves: a numerical experiment. *J. Fluid Mech.* **524**, 305–329.

Ubal, S., Giavedoni, M. D. & Saita, F. A. 2005*b* The formation of Faraday waves on a liquid covered with an insoluble surfactant: Influence of the surface equation of state. *Lat. Am. Appl. Res.* **35**, 59–66.

Ubal, S., Giavedoni, M. D. & Saita, F. A. 2005*c* The influence of surface viscosity on two-dimensional Faraday waves. *Ind. Engng Chem. Res.* **44**, 1090–1099.

Warner, M. R. E., Craster, R. V. & Matar, O. K. 2004 Fingering phenomena associated with insoluble surfactant spreading on thin liquid films. *J. Fluid Mech.* **510**, 169–200.

Wei, H.-H. 2007 Role of base flows on surfactant-driven interfacial instabilities. *Phys. Rev.* E **75**, 036306.

Wright, P. H. & Saylor, J. R. 2003 Patterning of particulate films using Faraday waves. *Rev. Sci. Instrum.* **74**, 4063–4070.